Tampere University of Applied Sciences

Applying The Multilayer Textile Conductor Technique To Improve The Wearable Passive RF Devices

Hau Ha

BACHELOR'S THESIS
October 2020

Energy and Environmental Engineering

ABSTRACT

Tampereen ammattikorkeakoulu
Tampere University of Applied Sciences
Energy and Environmental Engineering

AUTHOR: HA DUY HAU
Applying The Multilayer Textile Conductor Technique To Improve The Wearable Passive RF Devices

Bachelor's thesis 36 pages, appendices 6 pages
October 2020

The thesis aims to enhance the effectiveness of passive wearable RF device. The purpose of this thesis was to justify the utilization of multilayer of conductor structure to handle the challenge. It was hypothesized that lower reflection and higher gain can be achieved with higher amount of conductor layers. To prove the hypothesis, two two-port devices, the microstrip line and stepped impedance filter, were tested. Based on experience from previous research, EPDM rubber, copper-nickel conductive fabric and cotton fabric were chosen to construct the transmission line. In total, three samples for each device with three different number of conductor layers from one to three were conducted. During the experiment, the reflection coefficient (S11) and S21 of each sample structure, which represents the power transferred from Port 1 to Port 2 or gain, were measured by VNA (vector network analyzer). The parameters described performance of the RF passive devices and were compared in the end of the test. As the results, 3-layer conductor samples of both microstrip line and filter testing revealed the most optimal compared to those of one layer and two-layers.

The experiment procedure was performed at the Wireless Identification and Sensing Systems Research Group (WISE Group) of the Faculty of Medicine and Health Technology.

Key words: RFID, multilayer conductor, S parameter, wearable device

CONTENTS

1 INTRODUCTION

We are living in a rapidly changing world, where people are looking forward to environment-friendly and recycled products. The manufacture industry antennas and RF (radio frequency) circuits for wearable applications are not an exception. The bendable and stretchable materials such as conductive fabric, paper and EPDM cell rubber foam have been researched for wearable devices and body-worn wireless applications since they enable seamless cloth-integration. The products are advanced for their low price and environmental friendliness. Previously, there are many types of research about wearable antennas made by EPDM substrate and textile conductor for the wireless communication applications (Björninen 2018,706-709; Ma et al. 2018, 683-684; Le et al. 2019, 610-612; Björninen & Yang 2015, 794-797) However, the low conductivity of conductive fabric or lossy substrate may degrade the performance of the antenna, transmission line or low pass filter. It is a challenge to enhance the performance of the passive RF devices with a minor change of geometry of the device.

In order handle this challenge, we propose a new technique that is based on the utilization of multilayer of conductor made by conductive fabric. We employed two passive RF devices, namely the microstrip line and step impedance low pass filter as the candidate for testing this method. With this technique, we aim to reduce the attenuation of the microstrip line to upgrade the signal transmission. On the other hands, the gain of low pass filter at the bandpass and the attenuation at the stopband should be enhanced. This technique holds the promise to be low cost, speedy, uncomplicated and easily applicable. While the accuracy of this method is acceptable and meets the requirements of conscientious tests.

The implementation of the multiconductor method was conducted with some crucial procedures. First of all, we determined the materials for the transmission line and filters. Notably, the EPDM rubber is for substrate, the nickel conductive fabric is for signal and ground plane, and the cotton fabric is for the isolation between conductor layers. Next, we implemented and applied the multilayer of conductors on these passive devices. We conducted three samples for each device with

three different number of conductor layers (one layer, two layers and three layers). The geometry of the transmission line and filters is showed in previous research (Le et al. 2019). For multiconductor, we separated the conductor layers by a thin layer of cotton fabric and connected both ends by soldering. In the measurement step, we measured the reflection coefficient (S11) and S21 which represents the power transferred from Port 1 to Port 2 or gain by VNA (vector network analyzer). These parameters illustrate the performance of the RF passive devices, which will be described in detail in the next sections. We hypothesized that with higher conductor layers, the lower reflection coefficient and higher gain. Notably, the resistances from the multiple layers are in parallel; this could reduce the total resistance of the line. Hence, the total attenuation of the transmission line and low pass filter at passband will be decreased when the amount of conductor layer increased. All of the fabricated and measured steps were conducted at the Wireless Identification and Sensing Systems Research Group (WISE Group) of the Faculty of Medicine and Health Technology.

The thesis started with a short introduction in Chapter 1 could be followed by Chapter 2 will introduce the theoretical background of the microstrip lines, EPDM substrate, copper – Nickel conductor and transmission line. Next, scope of the work will be interpreted in Chapter 3. Chapter 4 will describe the more carefully the material used as well as the procedure of the laboratory experiment. The measurement results will be analyzed in Chapter 5 and further discussed in Chapter 6. Eventually, the thesis ends with a conclusion in Chapter 7.

2 THEORY BACKGROUND

In this chapter, we will have overview of the properties and characteristics of the flexible materials, namely, EPDM substrate and copper-Nikel. Besides, some theory background of the transmission line, S parameters and multilayer conductor transmission line structure are also summarized. Since EPDM will be played as the substrate and the copper- Nikel fabric is used as the conductor for the transmission line and the low pass filters, we will analyse the characteristics, the relative permittivity and loss tangent of the EPDM and conducting of the copper-nickel fabric, at high frequency. The electromagnetic wave propagation inside of the transmission line will be presented by the mathematic equation in the transmission line theory section. The S-parameters will be introduced in section 2.5. The meaning of each parameters will be discussed in this section. Finally, we will introduce new method to minimize attenuation for the passive circuit which is applying the multi-layer structure to the conductor of signal plane. Later this method will be applied for the transmission line and the passive pow pass filters.

2.1 EPDM substrate

EPDM (ethylene-propylene-diene monomer) is widely used to play an essential role in many major industries and trade fields. For example, in the automotive sector, EPDM is used extensively in components such as radiator and heater hoses, window and door seals, accumulator bladders, wire and cable connectors and insulators, and weather stripping. Moreover, widgets such as electrical power cables, white sidewalls of tires, roofing sheets, belting and sporting have also very high EPDM usage rates (Hua Zheng et al. 2004; Ismail et al. 2008; polymerdatabase.).

EPDM is an unsaturated polyolefin rubber which brings not only enormous economic benefit but also has many outdoor applications. It can resist to ageing, oxygen, UV and heat very well. Study reveals that the function temperature range is -45°C to +150°C (-50°F to +300°F) and up to +180°C (+355°F) in steam. Notably, EPDM is capable of enduring the high loading of fillers. The rubber shows

functional outstanding electric insulating capacity, low-temperature properties. Finally, EPDM is known for its good endurance to chemicals, and maybe the most water-resistant rubbers invented (Jiang Li et al., 2018; Ismail et al., 2008; polymerdatabase.).

On the other hand, there is still an unavoidable drawback. EPDM process unsatisfactory flame resistance. Additionally, the surface of the EPDM rubber has some inconvenient deficiency which is low adhesive properties. However, the most prominent disadvantage is low mechanical strength. Therefore, reinforcement agents are used to improve the property. For example, Carbon black is commonly used as a reinforcing agent in EPDM. Furthermore, to enhance the rubber properties hybrid and composite of EPDM rubber are usually constructed via vulcanizing such as EPDM/clay, EPDM/polypropylene, EPDM/OMMT, RPDM/HN,…. (Moraes 2007; Jiang Li et al. 2018; polymerdatabase.).

EPDM can be produced under both sponge and solid form. In this experiment, sponge, or foamed, EPDM rubber was used. Foamed EPDM has a porous characteristic with air pockets that is capable of holding air or permit its passage. Because of which, other than providing proper sealing and insulating, it as well provides excellent cushioning and, in this experiment, acts as a suitable substrate. To produce foamed EPDM, blowing agents are mixed in to generate bubble and create foam. The blowing agent can be mixed with various ratio resulting in different density combining different thickness depending on the desired application (Alanto; Melito 2019; Joeng et al. 2019; Chung et al. 1997.).

Figure 1. Example of EPDM (source: Industrial Gasket)

Recently, EPDM plays as a substrate for the wearable wireless communication devices namely antennas and passive circuits (Rizwan et al. 2015, 1-5; Koski et al. 2014). EPDM is a rubber-based material with light weight, excellent shock resistance high flexibility and easy attachment to any curved surface. Besides, the dielectric constant of EPDM is almost constant in a wide temperature range from - 40°C to +120°C which means that dielectric properties of material will be unchanged if used in extreme environments for example freezing cold or hot weather (Samuri 2009.). Hence, it is applicable for the wearable antennas. The dielectric constant and loss tangent of EPDM substrate are $\varepsilon_r = 1.53$ and $\delta = 0.01$ respectively.

2.2 Copper – Nickel conductor

Copper-nickel fabric is constructed with a metal surface of nickel and copper-plated on a base of polyester with nickel acts as a shield to prevent the oxidation of copper. The fabric is usually used as conductive fabric circuit, EMI shielding fabric, RFID shielding fabric, conductive cloth, anti-radiation fabric, phone signal shielding. In addition, it is also utilized in producing conductive foam and in computer signal lines, ribbon cable, etc. Copper-nickel duplicate fabric has shielding effect of 30 GHz~50 GHz in wide band and 6 GHz~12 GHz in wide frequency band. Copper-nickel is characterized by its great flexibility and resistance to tortuous as well as great electrical conductivity and anti-electromagnetic interference. Furthermore, by reflecting, absorbing on the basis of nature of the object as it encounters the wave, the fabric is able to provide good shielding effect (conductive-fabric; Yaping et al. 2017, Yaping et al. 2016.).

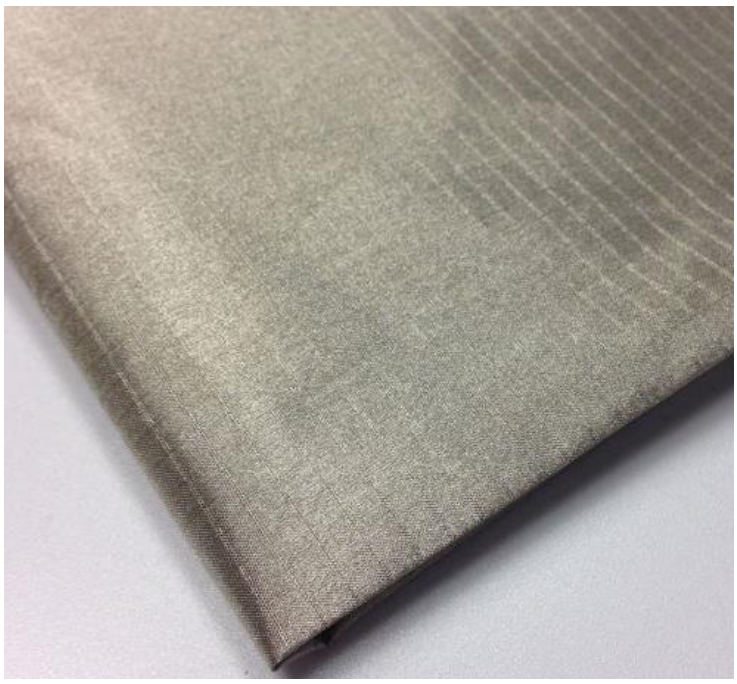

Figure 2. Sample of Coper-Nickel fabric (source: Aiwei Functional Textile Co., Ltd)

With least square estimation method, the previous research singled out the conductivity of the copper-nickel fabric that is 0.7×105 S/m from 0.2 GHz to 3 GHz. Hence, this conducting material is suitable for building up the wireless communication circuit, for instance, the low pass filter, balun and antennas. One of the key advantages of this materials is flexible and stretchable characteristic. It can be utilized to generate the wearable antennas or flexible RFID tag for biomedical applications. During this thesis work, the Copper-Nickel fabric was used as the conductor material for the signal plane and ground plane of the microstrip line and low pass filter. The fabric was attached to the EPDM substrate by using heat making the rubber to melt.

2.3 Microstrip line

The microstrip line, which is described as a planar transmission lines include the top is conductor installed on a ground plane composed of some dielectric layers or substrate with several relative permittivity'" E_r". It is considered the most popular planar circuit transmission lines, which can be scaled down, easy to use with passive or active microwave devices (Pozar 2011,147-149.) The air above the microstrip line and the substrate is an operational area of electromagnetic wave, which mutated by microstrip line. The dielectric substrates which are usually used

FR4, RT/Duroid, Arizona, Chandler, Rogers, Corporation other than the ground plane built with copper and nickel processing conductivity (Le 2018,14.).

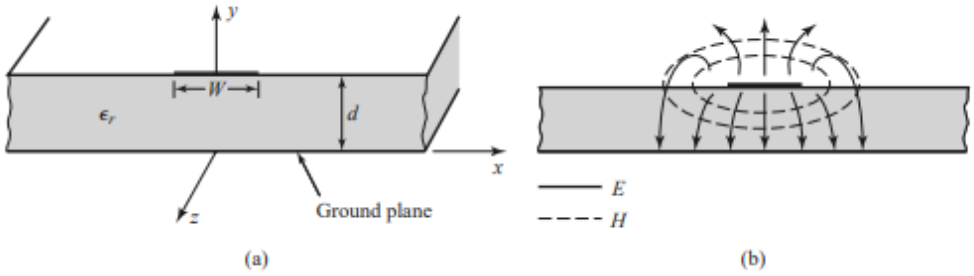

Figure 3. Microstrip transmission line. (a) Geometry. (b) Electric and magnetic field lines (Source: Pozar 2011,147-149)

Figure 3 illustrates the geometry and electric and magnetic field lines of the microstrip transmission line. In Figure 3, W stands for width of the conductor and d stands for the thickness of the substrate. These two parameters, along with the relative permittivity (ε_r) of the substrate directly affect the phase constant and characteristic impedance (Z_0) of the line. On the other hand, the signal attenuation is defined by the conductor thickness (t) and conductivity (σ) of the strip and ground conductors. Commonly, ε_r is usually used as a primary factor to achieve Z_0 that equals to the system impedance, which is normally 50 Ω, by enhancing the line width. As the result, the signal reflection as the beginning and the end of the line caused by impedance discontinuous can be diminished.

As the propagation in the microstrip line is in Transverse Electro-Magnetic (TEM) mode where all E-field lines run radially, while magnetic field lines run in circles around the center conductor. There is two way to express the phase velocity (formula 1 and 2). The phase velocity is expressed as:

$$v_p = \frac{c}{\sqrt{\varepsilon_{eff}}} \quad (1)$$

$$v_p = \frac{1}{\sqrt{LC}} \quad (2)$$

Where, c is the light speed (3x10^8 m/s), ε_{eff} is the microstrip relative dielectric constant, L is the inductance per unit length, and C is the capacitance per unit length.

The constant propagation β is achieved by formula 3 and the wavelength λ is achieved by formula 4 (El-Banna 2014)

$$\beta = k_0 \cdot \sqrt{\varepsilon_{eff}} \tag{3}$$

$$\lambda = \frac{c}{f\sqrt{\varepsilon_{eff}}} = \frac{v_p}{f} = \frac{\lambda_0}{\sqrt{\varepsilon_{eff}}} \tag{4}$$

In formula 4, λ_0 is the free space wavelength.

2.4 The equivalent circuit of microstrip line

The transmission line is assumed to be uniform, which means the cross-section of the line remains constant over the whole length in terms of the materials and geometry, in both geometry and materials in most theory and discussion regarding the topic. Transmission line is also represented as a conductor of which the homogeneity includes wavelength and the same size, shape, and distance of the line. Additionally, electrical characteristics and material of the conductors must be identical (Ron Schmitt 2002, 153; Le 2018, 11.).

The transmission lines possess leastwise two conductors. For instance, the ground plane and conducting plane function as the two conductors of the transverse electromagnetic (TEM) wave propagation. Hence, the transmission line can be expressed as a two-wire schematically. Whereas, the infinitesimal piece Δz of the transmission line (figure 1) is often demonstrated as a lumped-element circuit where (Pozar 2011, 48-51; Le 2018, 11.):

R = the resistance of limited conductivity,
L = self-inductance of two conductors,
G = shunt conductance per unit length
C = shunt capacitance per unit length
$i(z,t)$ = current at a specific point at a specific time on the line
V(z,t) = voltage at a specific point at a specific time on the line

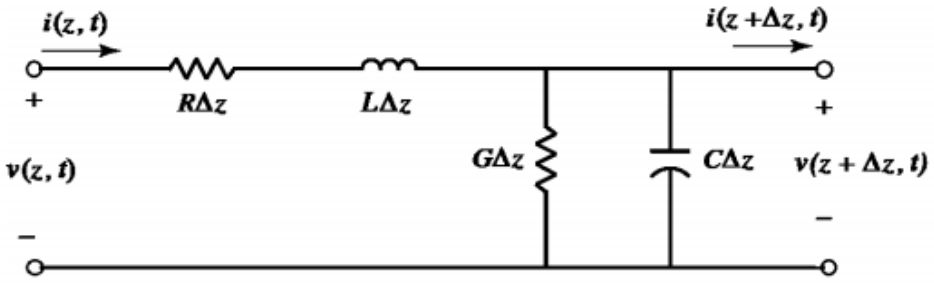

Figure 4. The lumped equivalent circuit of the transmission line

By applying the Ohm and voltage Kirchhoff's law for circuit, which was illustrated in Figure 4, voltage at a specific point at a specific time on the line can be demonstrated by the following equation (1):

$$v(z,t) = R\Delta z i(z,t) + L\Delta z \frac{\partial i(z,t)}{\partial t} v(z+\Delta z,t) \tag{5}$$

∆z is brought about nearly zero because line experiments are used within limits, which led to a different rearrange of formula 5:

$$\frac{\partial v(z,t)}{\partial z} = -Ri(z,t) - L\frac{\partial i(z,t)}{\partial t} \tag{6}$$

The current at a specific point at a specific time on the line expressed by Kirchhoff's law in figure 4:

$$i(z,t) = C\Delta z \frac{v(z+\Delta zt)}{\partial t} + G\Delta z v(z+\Delta zt) + u(z+\Delta zt) \tag{7}$$

When ∆z come forward to 0, The current at a specific point at a specific time on the line can be performed as:

$$\frac{\partial i(z,t)}{\partial z} = -Gv(z,t) - C\frac{\partial v(z,t)}{\partial t} \tag{8}$$

For the sinusoidal steady-state condition, with cosine-based phasors, formula 6 and 8 can be expressed as formula 9 and 10 respectively:

$$\frac{dV(z)}{\partial z} = -(R + j\omega L)I_{(z)} \quad (9)$$

$$\frac{dI(z)}{\partial z} = -(G + j\omega C)V_{(z)} \quad (10)$$

$v(z)$ and $i(z)$ wave equation was created base on the formula 9 and 10:

$$\frac{d^2V(z)}{dz^2} - \gamma^2 V_{(z)} = 0 \quad (11)$$

$$\frac{d^2I(z)}{dz^2} - \gamma^2 I_{(z)} = 0 \quad (12)$$

Where

$$\gamma = \alpha + j\beta = \sqrt{(R + j\omega L)(G + j\omega C)} \quad (13)$$

γ in formula 13 is the propagation constant acts as the function of frequency. The travelling wave of formula 5 and 6 is expressed in formula 14 and 15.

$$V_{(z)} = V^+ e^{-\gamma z} + V^- e^{\gamma z} \quad (14)$$

$$I_{(z)} = I^+ e^{-\gamma z} - I^- e^{\gamma z} \quad (15)$$

In which, the wave propagation in the +z(forward) and -z(reflected) direction are defined to be corresponding with $e^{-\gamma z}$ and $e^{\gamma z}$ in respect.

Z_o, which represent the characteristic impedance, can be defined by using the connection between the voltage and current on the line in formula 16.

$$\frac{{V_0}^+}{{I_0}^+} = Z_0 = \frac{-{V_0}^-}{{I_0}^-} \quad 16$$

Formula 14 and 15 can be reworded in another form as in formula 17. The formula is stating that both the incident and reflected waves are included in the total current of a transmission line.

$$I_{(Z)} = \frac{V_0^+}{z_0} e^{-\gamma z} - \frac{V_0^-}{z_0} e^{\gamma z} \quad 17$$

From equation (17), it can be seen that the total current of a transmission line consists of both incident and reflection waves. As a consequence, the relationship between the reaflected waves from the load $(V^-)e^{\gamma z}|_{Z=0} = V^-$ and the incidented wave to the load $(V^+)e^{-\gamma z}|_{Z=0} = V^+$ can be found.

$$\Gamma = \frac{V^-}{V^+} = \frac{Z_L - Z_0}{Z_L + Z_0} \quad 18$$

where Z_L presents the impedance load impedance and the Z_0 is the characteristic impedance of the transmission line

2.5 Scattering parameters

The S-parameters, or scattering parameters, are particular parameters which are essential in RF devices such as linear circuit (Lehtovuori et al 2004), active circuits, transmission lines and antennas or electric network (Le 2018, 18). S-parameters define the input-output relationship between ports as well as propagation of energy through an electrical network. The relationship is described in Figure 5. There are three approaches by which S-parameters can be calculated (Lehtovuori et al 2004.):

- Physic by solving Maxwell's equation
- Linearizing the semiconductor equations
- The matrix analysis of the linear equivalent circuit

S-parameters shows various benefits as there are alternatives on how to apply the parameter. For instance, S-parameter can be used for measuring device or designing system. In addition, when the RF devices or electric network are infused energy and high frequency presented, as an alternation for voltages and currents, s-parameters can be used for determining and expressing a network in terms of frequency versus amplitude wave (Lehtovuori et al 2004.)

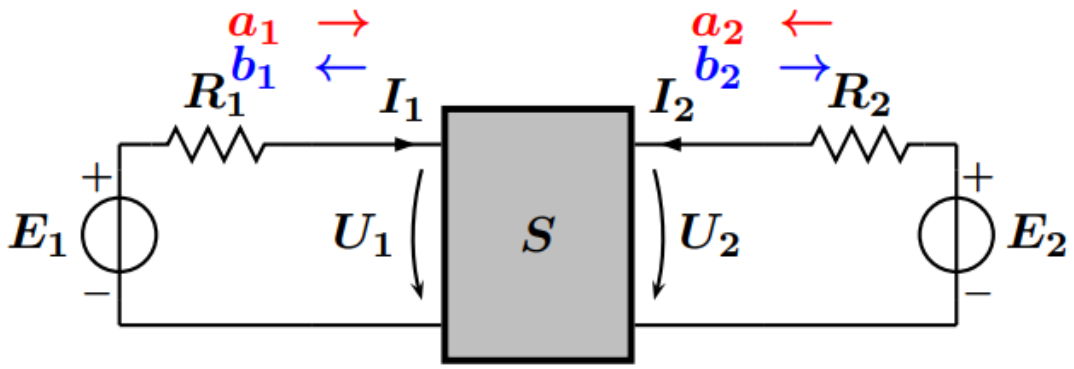

Figure 5. The definition of scattering parameters (Source: Lehtovuori et al 2004)

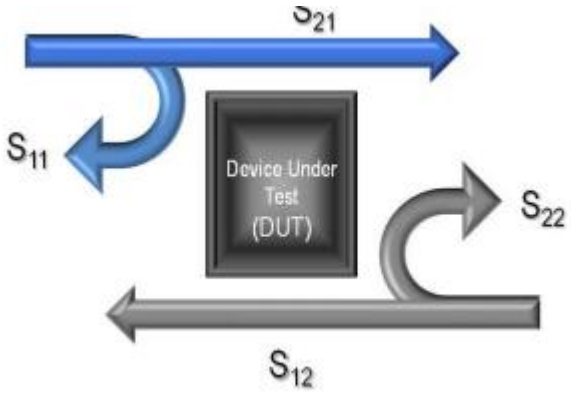

Figure 6. The S-parameter matrix (Lehtovuori et al 2004)

S-parameter matrix in Figure 6 demonstrates the reflection coefficient and directional transmission of four-port with 2 input ports and 2 output ports in the system. S_{11} is the input port voltage reflection which shows the coefficient at port 1 and represents the amount of energy reflected to port 1. S_{11} is often used to studied the reflection coefficient of a network. S_{22} is defined as the output reflection voltage coefficient which indicates the amount of energy reflected to port 2. S_{21} is the forward voltage transmission from port 2 to port 1 which demonstrates the power transfer efficiency from port 2 to port 1. Notably, in some cases, S_{21} also represents the gain, which describes the transmission quality from the start point to the end point of a transmission line. Lastly, S_{12} is the reverse voltage transmission from port 1 to port 2 (Le 2018, 18; Lehtovuori et al 2004; Garade 2018.).

In RF circuit, impedance is an importance term. Hence, the return loss is used to described the loss of power in signal, which is returned or reflected as the result

of impedance mismatch (Electricsnotes; Bird 2009, 166-167) The Positive Return loss (RL) is expressed by formula 18 below:

$$RL = 10log_{10}\left(\frac{P_{in}}{P_{ref}}\right)dB \tag{19}$$

On the other hand, negative RL is expressed by formula 19 below:

$$RL = 10log_{10}\left(\frac{P_{ref}}{P_{in}}\right)dB \tag{20}$$

2.6 Multilayers conductors of transmission line

According to skin depth effect (RFcafe 2006), the current inside of the transmission line (microstrip line) flows on the surface of the conductor layer at higher frequency. The current density inside of the transmission line is decreased exponentially with penetration into the conductor, declining to 1/e of its surface value at one skin depth

$$\delta = \sqrt{\frac{2}{\omega\mu\sigma}} \tag{21}$$

where δ is the skin depth, μ is conductor magnetic permeability, σ is bulk conductivity and ω is radian frequency.

The current density of a plane wave inside of the thick conductor can be expressed (Rautio.j. C. 2003):

$$J(z) = J_0 e^{-\frac{z}{\delta}}(\cos\left(\frac{z}{\delta}\right) - jsin\left(\frac{z}{\delta}\right)) \tag{22}$$

where J_0 is the current density at surface of conductor, perpendicular to the z axis.

The surface impedance Z_s of the thick conductor of a plane wave propagating along the z axis into the conductor

$$Z_s = \sqrt{\frac{j\omega\mu}{\sigma}} = (1+j)\sqrt{\frac{\omega\mu}{2\sigma}} \tag{23}$$

On the other hands, the surface impedance can be found by [8]

$$Z_s = -jZ_0 \cot kt \tag{24}$$

Where

$$k = \sqrt{-j\omega\mu\sigma} = (1-j)\sqrt{\frac{\omega\mu\sigma}{2}} = (1-j)\frac{1}{\delta} \tag{25}$$

The surface impedance is also expressed as:

$$Z_s = (1-j)R_{RF}\sqrt{f}\left((1-j)R_{RF}\sqrt{f}\frac{1}{R_{DC}}\right) \tag{26}$$

Where

$$R_{DC} = \frac{1}{\sigma t} \tag{27}$$

$$R_{RF} = \sqrt{\frac{\pi\mu}{\sigma}} \tag{28}$$

f is the frequency (Hz)

from equation (25), the Z_s= R_{DC} at low frequency and $Z_s = (1+j)R_{RF}\sqrt{f}$ at higher frequency.

From the equation of the surface impedance, the thickness of the conductor does not impact on the total impedance of the transmission line. As our approach, when we increase number of layers by stacking all of conductors separately. The total resistance of the line may decrease based on Ohm's law.

The main goal of using multilayer conductor is to increase the RF performance of the microstrip line and passive circuits, especially, which is passive stub filter. It follows from the laws of electromagnetism and states that no matter how thick is conductor, most of the current will flow only in the surface layer of the conductor (and thus defines its resistance) and the thickness of the "surface layer" gets

thinner as the frequency increases. As a result, making the conductor “too thick” does not have an effect on the resistance because the current flow in the surface layer anyway. However, when we put several conductors in parallel, the same phenomenon occurs in parallel (or stacked conductors) conductors separately and according to Ohm's law, the resistance is reduced exactly as you have explained in this section. Specifically, it is hypothesized that the increasement of the number of the conductor layers leads to the lower attenuation or loss in the microstrip line.

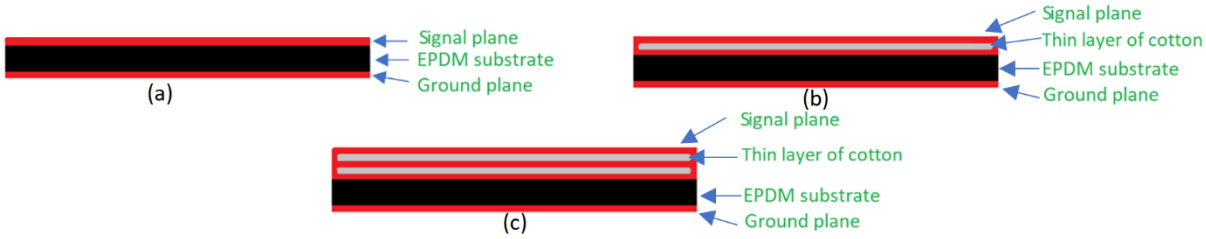

Figure 7. The geometry of transmission line with the one layer (a), two layers (b) and three layers (c) of conductor.

Figure 7 demonstrates the structure of the transmission line with various number of conductor layers. Basically, we constructed the transmission lines with three elements namely, signal plane made by copper, 3 mm thickness EPDM substrate and ground plane made by copper. When increasing the number of conductor layers as two layers and three layers, we separated by sandwiching thin layer of cotton fabric between each layer as Figure 7 (b) and (c). At the both ends of the transmission line; the conductors were connected by soldering. After that, the SMA (Subminiature version A) connectors were attached at both ends of the microstrip line for measuring purpose. The main idea is that on each layer the current is packed to a limited thickness near the top and bottom surface this corresponds to a series resistance. When the resistances from the multiple layers are in parallel this could reduce the total resistance of the line.

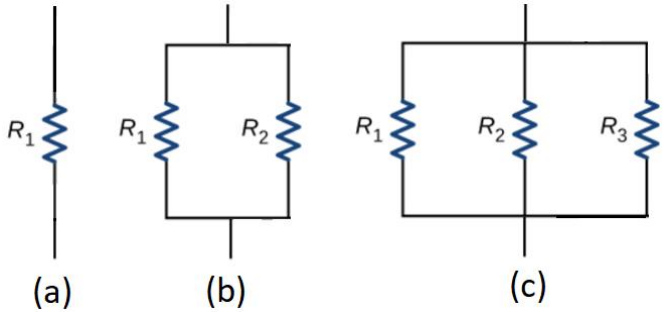

Figure 8. The equivalent resistance circuit of one layer (a), two layers (b) and three layers (c) of conductor.

As be shown in Figure 8, the resistance of first layer is R1, second layer is R2 and third layer is R3. Since the length and material of the conductor are identical, it is assumed that R1= R2 = R3 is the total resistance of one layer, two layers and three layers of conductor are (Preston, D. C., & Shapiro, B. E 2012.).

$$\mathrm{Rtotal}_{1\mathrm{L}} = R_1,\ \mathrm{Rtotal}_{2\mathrm{L}} = \frac{R_1.R_2}{R_1+R_2} \text{ and } \mathrm{Rtotal}_{3\mathrm{L}} = \frac{R_1.R_2.R_3}{R_1+R_2+R_3}$$

It can be observed that $\mathrm{Rtotal}_{1\mathrm{L}} > \mathrm{Rtotal}_{2\mathrm{L}} > \mathrm{Rtotal}_{3\mathrm{L}}$ or the decrement of the resistance is corresponding to the increment of conductor layer number. Thus, we predicted that with higher number of conductor layers, the RF passive devices such as the microstrip line and step impedance low pass filet possess higher RF performance.

3 SCOPE OF THE WORK

The thesis aims to enhance the performance of passive wearable RF devices by applying the multilayer structure for the conductor of signal plane. It can be explained that each conductor layer is corresponding to a resistor. Additionally, the multilayer conductor structure can be assumed as parallel resistors. Eventually, it leads to the total resistance of the passive RF device decreased and the RF performance namely reflection coefficient improved, and signal loss decreased. In this thesis, we used 2-port devices namely, the microstrip line and stepped impedance filter to test this hypothesis. Our expectation is that the attenuation of the transmission line will decrease corresponding to the increment of the number of conductor layer. For the low pass stepped filter, the gain of the low frequency signal will be enhanced and the attenuation will be improved at higher frequency. Each device was constructed with three samples which possess variation of a number of conductor layers (one layer, two layers and three layers). The main materials of these devices were textile materials namely EPDM robber for the substrate and nickel conductive fabric for the conductor which are suitable for wearable wireless applications through this experiment, we want to prove the feasibility of the multilayer technique.

4 MATRIALS AND METHODS

4.1 Practical structure samples

The basic structure of the microstrip line and low pass filter is composed of two conducting layers namely, a top layer and the bottom layer and substrate layer. The top layer acts as the main signal called the signal plane and located on the top. This layer was constructed of Coper-Nickel plate. The bottom layer was made of the same material with signal plane, called the ground plane. In other test structures where multilayer is constructed, there are as well thin cotton sandwiched in between the layers to insulate the layers. The layers were attached by a type of super glue. At both end, all of layer was connected by soldering and connected to the 50Ω SMA connectors. It is noted that the distance between the starting point of the microstrip line and the SMA connector was minimized as small as possible as Figure 10. It can mitigate the extra phase shift from both sides, hence, it can improve the accuracy of the measurement results.

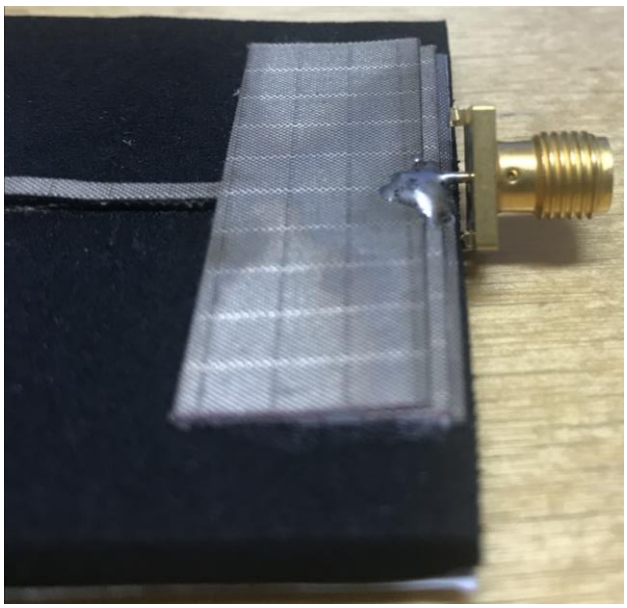

Figure 9. One end of the low pass filter

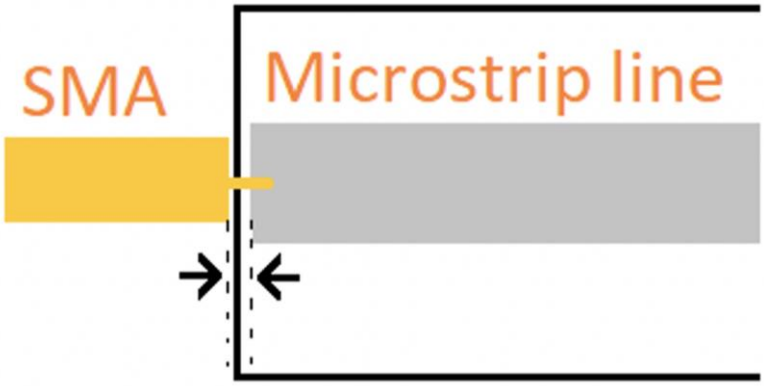

Figure 10. The top view of the microstrip line

4.1.1 The microstrip line

This experiment aims to study the S parameters of the test structures, which is configured as microstrip lines by using a VNA system. There were three types of the test structures, 1-layer, 2-layer and 3-layer constructed as described above. The 1-layer structure was constructed the same as a basic test structure with signal plane, EPDM substrate and ground plane without the cotton layer. Whereas, the 2-layer, 3-layer were constructed with thin layers of cotton placed in between several main signal planes (Figure 11). The length of the EPDM substrate is approximately 8.2 cm, and it is 20mm thick.

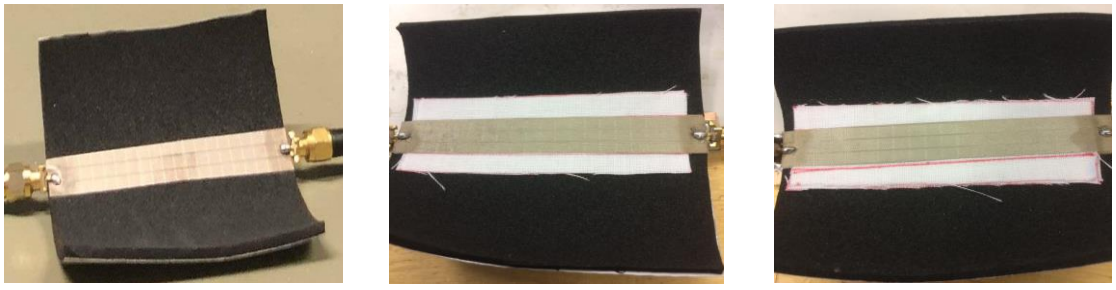

(a) (b) (c)

Figure 11. Micrstrip line with one (a), two (b) and three (c) layers of conductors

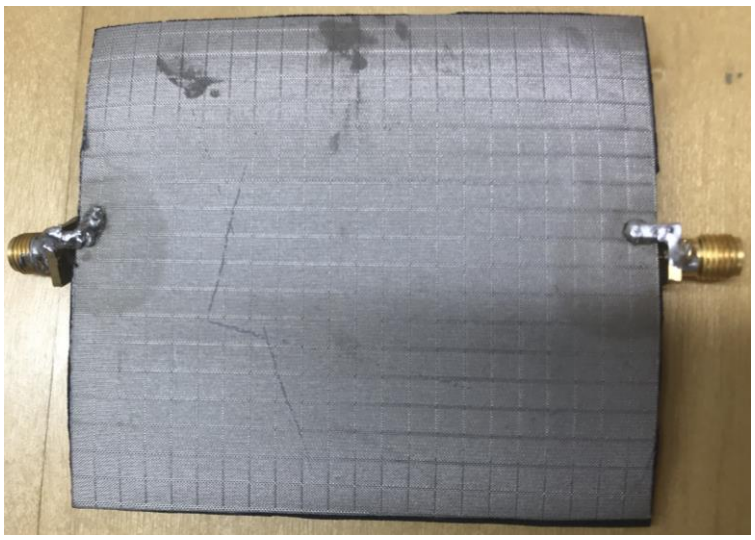

Figure 12. The ground plane of the microstrip line

4.1.2 Stepped impedance filter

Stepped impedance filter is another typical class of microwave transmission line filter (Pozar, D. M. 2011.). Same as the analyses performed for microchip lines, there were as well three types of the test structures, 1-layer, 2-layer and 3-layer. (Figure 13) The low pass stepped impedance is a RF device that filter the signal at high frequency and allows the low frequency signal transmitted from port 1 to port 2. Stepped impedance filter is more straightforward in structure and design. All the filters were designed for 50 Ω system impedance. Of which, the pass-band corner frequency with 3-dB attenuation at 1 GHz and stop-band starting frequency with more than 15 dB attenuation at 2 GHz.

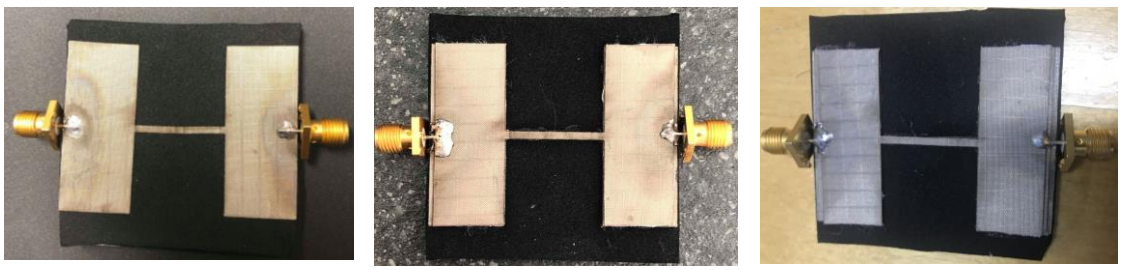

(a) (b) (c)

Figure 13. The low pass filters with one (a), two (b) and three (c) layers of conductors

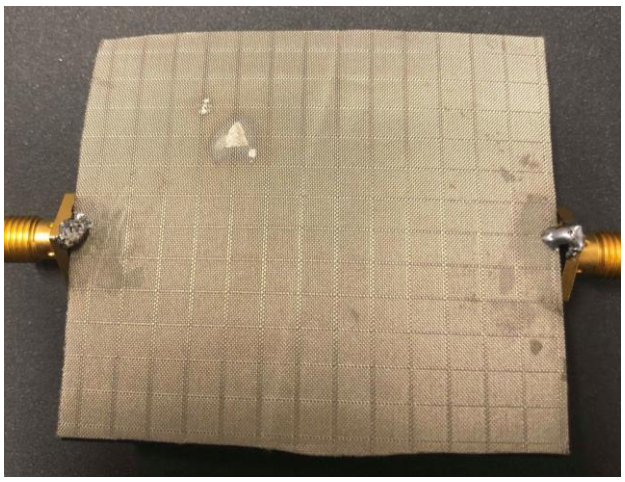

Figure 14. The bottom size of low pass filter

4.2 Measurement setup VNA

Vector network analyser, also known as VNA, was utilized to achieve the S parameters for the microstrip transmission line. In prior to the primary measurement, it was essential to calibrate the device due to various factors that affect the result. For example, the common factors are temperature, environment and measuring cable etc. (National Instrument 2020.) Hence, calibration was necessary to get rid of the losses and undesired signals from the SMA connectors and the measuring cables. As a result, the outcome would be the results of DUT (device under test) itself. The calibration box of Agilent 85093-60007 was used in this experiment (Spurlock 2017.).

To transmit the signal from the microstrip transmission line samples to the VNA, two cables were connected to the SMA connectors of the samples. The other side of the cables were connected to the VNA. It was noted that the SMA connectors had to be attached by a suitable force. This setup was used to measure the S parameter of the microstrip transmission line samples with the high-frequency application (Figure 15) and of the stepped impendence low-pass filter (Figure 15).

Figure 15. The microstrip transmission line (left side) and low pass filter (right side) measurement setup

5 MEASUREMENT RESULTS

In this section, the performance of the transmission line and low pass filer are described by the so-called S-parameters also known as scattering parameter. It shows the relationship between the ports of the measurement models are presented (Garade 2018). In this experiment, the S-parameters of microstrip line and low pass filter were automatically measured by the VNA system. The measurement results include the S_{11} and S_{21} which stand for the reflection confident and insertion loss respectively.

5.1 Microstrip line

5.1.1 Reflection coefficient S_{11}

Figure 16 symbolizes S_{11} of 1-layer, 2-layer and 3-layer model. In the first observation, it is not difficult to recognize that the yellow line, which represents the s parameters of 3 layers model is less dislocated from the standard -30 dB from the begin.

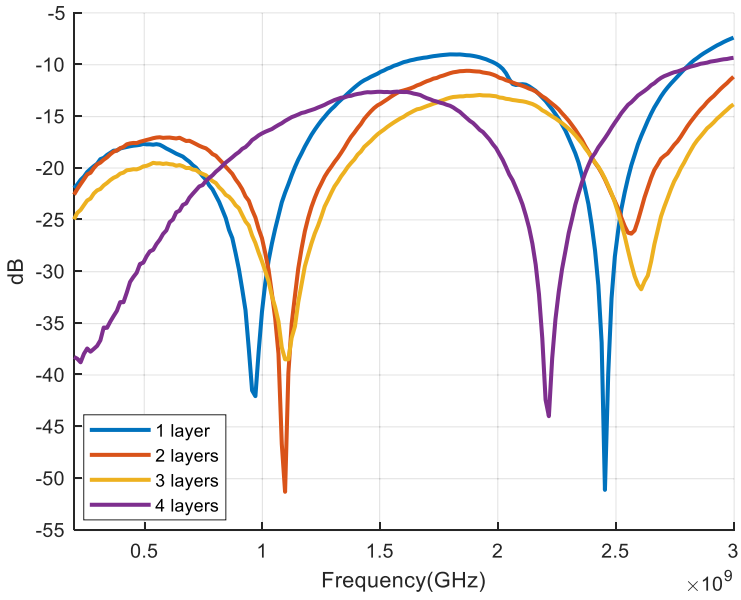

Figure 16. The S parameters S_{11} reflection coefficient of microstrip line of experimental samples

The first low-lying area, at Frequency from 0.8Hz to 1.2Hz (figure 15), the s parameter of the 2 layers have the lowest point around -51db at 1.1hz. The S11 measurement of 1 layer and 3 layers model are lower than those of 2 layers model respectively around 9 dB and 12 dB. On the other hand, the second low-lying area at Frequency from 2.2hz to 2.7hz the 1 layer has lowest S_{11} which is as well roughly -51dB at 2.45 Ghz. The S_{11} of the layer is 25 dB and 20 dB higher than 2-layer and 3-layer, respectively.

5.1.2 S_{21}

Figure 17 symbolize the S parameter of S_{21} of 1-layer, 2-layer and 3-layer model. Overall, the s parameter of 1-layer model fluctuates the most significantly. On the other hand, 2-layer and 3-layer's S parameter seem to be more stable. The main idea is to achieve S21 the closer to 0 the less loss hat device contains (Antenna Theory). At Frequency 3 GHz, the 1-layer reached the highest at -3 dB, which is 1.2 dB higher than the 2-layer model and 1.6 dB higher than the 3-layer model. At the start point of the figure 19, the yielded results of 2- and 3-layer model were a similar result. However, the 3-layer model had a better performance from frequency 1.5 GHz to 3 GHz.

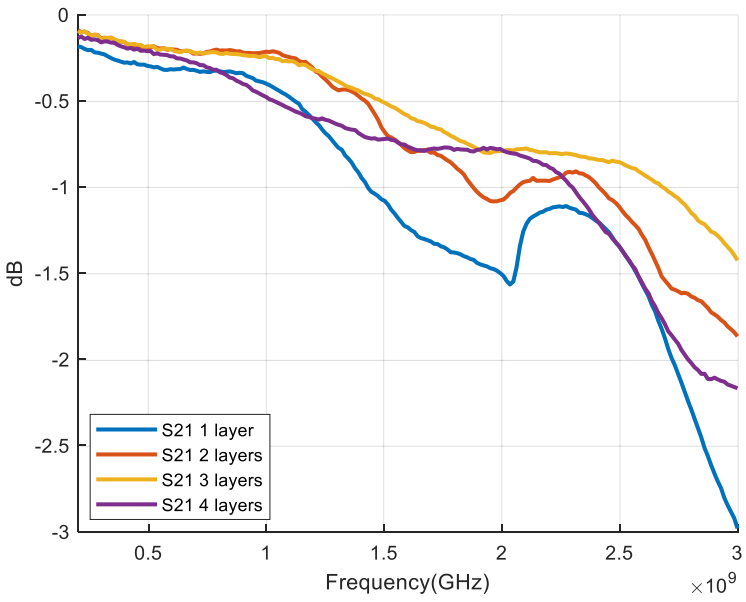

Figure 17. The S parameters S_{21} transmission coefficient of microstrip line of experimental samples

5.2 Stepped impedance filler

5.2.1 S_{11}

Figure 18 represent the S_{11} S parameter of 1-layer, 2-layer and 3-layer model. Generally, the 3-layer model reveals pre-eminence compare with 1-layer and 2-layer model, especially from frequency 0 GHz to 1.5 GHz. However, from frequency 1.5 GHz to 3 GHz its S-parameter almost equal to the 2-layer model. In addition, the 3-layer starts at -28 dB, which is very close to the standard of S_{11} (-30 dB), 3 dB higher than the 2-layer model and 5 dB higher than the 1-layer model.

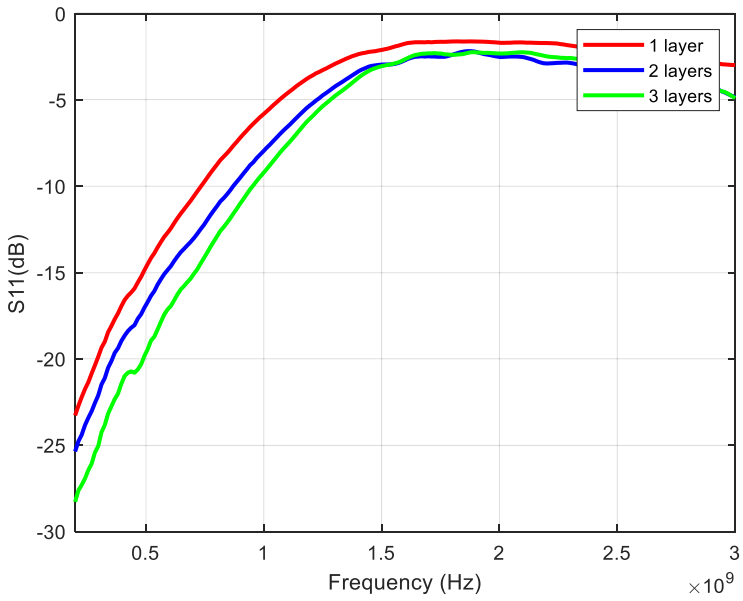

Figure 18. The S parameters S_{11} reflection coefficient of stepped impedance low pass filter of experimental samples

5.2.2 S_{21}

Figure 19 shows the S_{21} S parameter of 1-layer, 2-layer and 3-layer model. In general, although all 3 models started at the same point, the 1-layer model still shows the worst performance compare with 2-layer and 3-layer model that it rapidly decreases and finally ends at -27 dB. Meanwhile, the 2-layer and 3-layer model do not show a significant difference from Frequency 0 GHz to 1.8 GHz. Additionally, from 1.8 GHz to 3 GHz, the 2-layer model has little fluctuation. However, it ends at the same point at the 3-layer model (-22.5 dB).

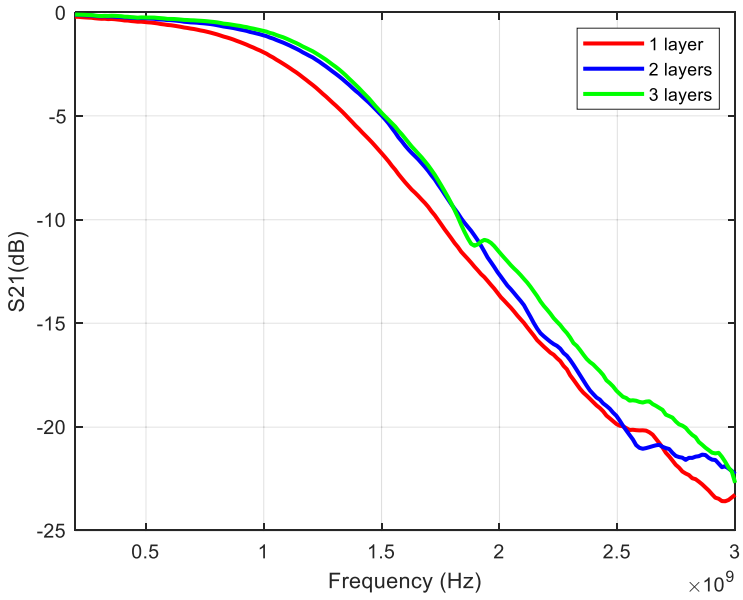

Figure 19. S parameters S_{21} transmission coefficient of stepped impedance low pass filter of experimental samples

6 DISCUSSION

The main materials of these devices were textile materials namely EPDM robber for the substrate and nikel conductive fabric for the conductor which are suitable for wearable wireless applications. The parameters used to indicate the RF performance of the devices are S parameters namely, S_{11} and S_{21}. S_{11} is the reflection coefficient which shows the amount of signal reflected from port 1 and the power transferred from Port 1 to Port 2 or gain is illustrated by S_{21}. The frequency range of the measurement of the transmission line is from 0.2 GHz to 2 GHz and those of the low pass filter is 0.2 GHz to 1 GHz for the band pass and 1 GHz to 3 GHz is for stop band.

The microstrip line testing provides data concerning S_{11} and S_{21}. The result from 3-layer testing revealed the most optimal S_{11} and S_{21} compared to 1-layer and 2-layer. S_{11} represents the reflection coefficient and indicate the power loss of the antenna. Studies have shown that to have an ideal reflection, S_{11} should to be as close -30 dB as much as possible. This statement can be explained by an example with formula 15 assuming the power input is 10 watt and the return loss S_{11} is -30 dB.

$$RL = -30dB = 10log\left(\frac{P_{ref}}{10}\right) \Rightarrow P_{ref} = 0.01 = 1\%$$

The example indicated that with S_{11} equal to -30dB, there would be only 1% incident power is reflected back to the source of the device. The result from 3-layer testing showed that 3-layer sample had the closed S11 to -30dB, therefore, it was recognized as the most ideal among the sample in term of power loss.

On the other hand, S_{21} is insertion loss. S_{21} represents the power transferred from Port 1 to Port 2. This is a good way to describe its physical expression when the two-port device is a cable or some sort of attenuator. This is the ratio of the incident wave at port 2 and the power wave leaving port 1. S_{21}=0 dB implies that all the power delivered to port 1 ends up at the terminals of port 2 (Bockelman & Eisenstadt 1995,1530-1539.). The closer to zero S_{21} is the better. Compare to 1 layer and two-layer structure, and three layers gave the best result. Stepped impedance low pass filter provides data concerning S_{11} and S_{21}. The same as the

microstrip line RF device, the three-layer structure still showed the most optimal in both S_{11} and S_{21}.

7 CONCLUSION

According to the measurement results, it can be observed that the increment of the conductor layers leads to the superior performance of the passive RF devices. To be more specific, with lower S_{11} and higher S_{21}, the result from 3-layer conductor sample of the microstrip line and filter testing revealed the most optimal compared to those of one layer and two-layers. Meanwhile, the 2-layer conductor is the second best compared one-layer conductor samples. The low pass filter provided quite satisfying results. In the, by applying multiconductor technique, the loss of signal at the band pass (0.2 GHz – 1 GHz) filter is declined according to increment of conductor layer number. The attenuation at the stop band (1 GHz - 3 GHz) is also improved.

One of the most challenging in this thesis is the fabrication process. Because the low pass filter layout consists of some minor and edgy area, manual implementation will cause some errors that negatively impacts the final measurement results. To deal with that issue, the shape of the signal plane of the devices was formed by the laser cutter with high precision. Besides, generating multilayer samples was also a difficulty procedure; we needed to rigorously stack over the conductor layers to each other without changing the original sample layout. To handle this challenging, we decided to fabricate three samples for each type of transmission line and filter. Although this step is time-consuming, it provided accurate results.

In term of future work, the multilayer conductor technique can be applied for wearable antenna development. By this approach, the antenna gain, and reflection coefficient can be upgraded. Notably, the wearable RFID tag antenna is an excellent idea to apply. We could improve the achievable read range of the RFID tag with a higher number of conductor layers.

REFERENCES

All About Vector Network Analyzer Calibration. 2020. Article. Read 31.05.2020. Source: https://www.ni.com/fi-fi/innovations/videos/10/all-about-vector-network-analyzer-calibration.html

Alanto EPDM Sponge (Closed Cell). Article. Read 25.05.2020. Source: https://www.alanto.co.uk/epdm-closed-cell-sponge

Björninen, T. (2018). Comparison of three body models of different complexities in modelling of equal-sized dipole and folded dipole wearable passive UHF RFID tags. Applied Computational Electromagnetics Society Journal, 33(6), 706-709.

Björninen, T., & Yang, F. (2015). Low-profile head-worn antenna with a monopole-like radiation pattern. IEEE antennas and wireless propagation le ters, 15, 794-797.

Bockelman, D. E., & Eisenstadt, W. R. (1995). Combined differential and common-mode scattering parameters: Theory and simulation. IEEE transactions on microwave theory and techniques, 43(7), 1530-1539.

Bird, T. S. (2009). Definition and misuse of return loss [report of the transactions editor-in-chief]. IEEE Antennas and Propagation Magazine, 51(2), 166-167.

Chung, B., Bruce, M., Ivan, P. 1997. EPDM Compositions And Process For Producing The Same. Boston: Carbot Corporation.

EPDM - ETHYLENE PROPYLENE DIENE RUBBE. Article. Read 25.05.2020, Source: https://polymerdatabase.com/Elastomers/EPDM.html.

El-Banna, A. 2014. Power Dividers and Directional Couplers. Lecture. Benha University: Faculty of Engineering at Shoubra.

Garade, M. 2018. What are S-parameter?. Article. Read 20.07.2020. https://www.everythingrf.com/community/what-are-s-parameters

Ismail, H., Pasbakhsh, P., Fauzi, M. A., & Bakar, A. A. (2008). Morphological, thermal and tensile properties of halloysite nanotubes filled ethylene propylene diene monomer (EPDM) nanocomposites. Polymer Testing, 27(7), 841-850.

Koski, K., Lohan, E. S., Sydänheimo, L., Ukkonen, L., & Rahmat-Samii, Y. (2014, September). Electro-textile UHF RFID patch antennas for positioning and localization applications. In 2014 Ieee Rfid Technology and Applications Conference (Rfid-Ta) (pp. 246-250). IEEE.

Le, D., Kuang, Y., Ukkonen, L., & Björninen, T. (2019). Microstrip transmission line model-fitting approach for characterization of textile materials as dielectrics and conductors for wearable electronics. International Journal of Numerical Modelling: Electronic Networks, Devices and Fields, 32(6), e2582.

Le, D. (2018). Computing the Relative Permittivity and Loss Tangent of Substrates by the Numerical Model of a Microstrip Transmission Line (Master's thesis).

Le, D., Ukkonen, L., & Björninen, T. (2019, December). Dual-ID Headgear UHF RFID Tag with Broadside and End-Fire Patterns based on Quasi-Yagi Antenna. In 2019 IEEE Asia-Pacific Microwave Conference (APMC) (pp. 610-612). IEEE.

Lehtovuori, L. Costa, M. Honkala, A. Kallio, A. Kivikero, J. Virtanen: Piirisynteesi, Yliopistopaino, 2004.

Li, Y., Wang, X., Pan, Z., Su, Y., Liu, Z., Duan, J., & Li, Y. (2019). Analysis of shielding effectiveness in different kinds of electromagnetic shielding fabrics under different test conditions. Textile Research Journal, 89(3), 375-388.

Li, Y., Wang, X., Pan, Z., Su, Y., & Liu, Z. (2016, August). Analysis of shielding effectiveness in different kinds of electromagnetic shielding fabric in the wide frequency of 1GHz~ 18GHz. In 2016 Progress in Electromagnetic Research Symposium (PIERS) (pp. 1838-1842). IEEE.

Ma, S., Ukkonen, L., Sydänheimo, L., & Björninen, T. (2018, July). Dual-Layer Circularly Polarized Split Ring Resonator Inspired Antenna for Wearable UHF RFID Tag. In 2018 IEEE International Symposium on Antennas and Propagation & USNC/URSI National Radio Science Meeting (pp. 683-684). IEEE.

Melito, S. 2019. Solid Rubber vs. Sponge Rubber: What's the Difference?, Article, Read 25.05.2020, Source: https://www.elastoproxy.com/solid-rubber-vs-sponge-rubber/

Nickel Copper Coated Conductive Fabric Circuit For Electrical Products. Article. Read 01.06.2020. Source: http://www.conductive-fabric.com/sale-8234197-nickel-copper-coated-conductive-fabric-circuit-for-electrical-products.html

National Instrument (2020), All About Vector Network Analyzer Calibration, Read 14.05.2020, Source: https://www.ni.com/fi-fi/innovations/videos/10/all-about-vector-network-analyzer-calibration.html

Pozar D. Microwave Engineering, Fourth Edition, 2011.

Preston, D. C., & Shapiro, B. E. (2012). Electromyography and neuromuscular disorders e-book: clinical-electrophysiologic correlations (Expert Consult-Online). Elsevier Health Sciences, page 603-605

Rizwan, M., Khan, M. W. A., Sydänheimo, L., & Ukkonen, L. (2015, November). Performance evaluation of circularly polarized patch antenna on flexible EPDM substrate near human body. In 2015 Loughborough Antennas & Propagation Conference (LAPC) (pp. 1-5). IEEE.

RFcafe (2006). Skin Depth (aka Skin Effect) as a Function of Frequency, Pemeability, & Conductivity. Read 30.11.2020 ,Source: http://www.rfcafe.com/refeences/electrical/skin-depth.htm

Rautio, J. C., & Demir, V. (2003). Microstrip conductor loss models for electromagnetic analysis. IEEE transactions on microwave theory and techniques, 51(3), 915-921.

Samsuri, A. (2009). An introduction to polymer science and rubber technology. Shah Alam, Selangor: Pusat Penerbitan Universiti, Universiti Teknologi MARA, 2009.

Sang, J. S., Park, E. Y., Lim, S. W., Park, S., & Oh, K. W. (2019). Performance of bio-ethylene propylene diene monomer (bio-EPDM) foam with mixed chemical and encapsulated blowing agents. Fashion and Textiles, 6(1), 21.

Schmitt, R. (2002). Electromagnetics explained: a handbook for wireless/RF, EMC, and high-speed electronics. Elsevier,153.

S-parameter. Article. Read 30.06.2020. http://www.antenna-theory.com/definitions/sparameters.php

Spurlock, J. 2017. Improving VNA measurement accuracy with quality cables and adapters. Article. Read 31.05.2020. Source: https://www.tek.com/blog/improving-vna-measurement-accuracy-quality-cables-and-adapters

Tektronix (2017). Improving VNA measurement accuracy with quality cables and adapters. Read:14.05.2020. Source: https://www.tek.com/blog/improving-vna-measurement-accuracy-quality-cables-and-adapters.

What is Return Loss. Article. Read 30.06.2020. https://www.electronics-notes.com/articles/antennas-propagation/vswr-return-loss/what-is-return-loss.php

Zheng, H., Zhang, Y., Peng, Z., & Zhang, Y. 2004. Influence of clay modification on the structure and mechanical properties of EPDM/montmorillonite nanocomposites. Polymer Testing, 23 (2), 217-223.

APPENDICES

Appendix 1. Layout of signal plane of microstrip line

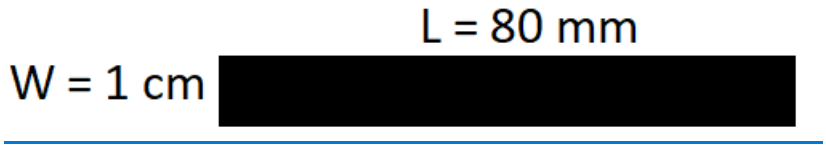

Appendix 2. Layout of signal plane of low pass filter

W_1 = 43 mm	L_1 = 16 mm	L_2 = 21 mm	W_2 = 2mm

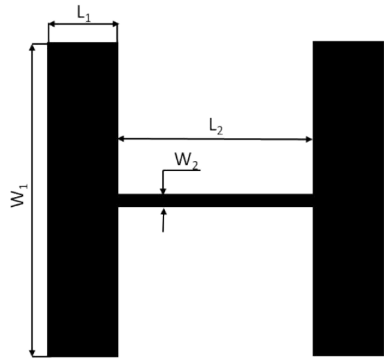

Appendix 3. Data processing: Importing measured data and extracting data to S parameters

```
close all
clc

% Importing data
data_1_layer = read(rfdata.data,'1layertxline.s2p');
data_2_layer = read(rfdata.data,'2layer1.11cm.s2p');
data_3_layer = read(rfdata.data,'3layer1.11cm.s2p');

% Extracting S parameters
S_1_layer = data_1_layer.S_Parameters;
S_2_layer = data_2_layer.S_Parameters;
S_3_layer = data_3_layer.S_Parameters;

f = data_1_layer.Freq; %GHz

s11_1_layer= S_1_layer(1,1,:); s12_1_layer = S_1_layer(1,2,:);
s21_1_layer= S_1_layer(2,1,:); s22_1_layer = S_1_layer(2,2,:);
s11_2_layer= S_2_layer(1,1,:); s12_2_layer = S_2_layer(1,2,:);
s21_2_layer= S_2_layer(2,1,:); s22_2_layer = S_2_layer(2,2,:);
s11_3_layer= S_3_layer(1,1,:); s12_3_layer = S_3_layer(1,2,:);
s21_3_layer= S_3_layer(2,1,:); s22_3_layer = S_3_layer(2,2,:);

Gma_m_1_layer = 10*log10(powergain(S_1_layer,'Gmag'));
Gma_m_2_layer = 10*log10(powergain(S_2_layer,'Gmag'));
Gma_m_3_layer = 10*log10(powergain(S_3_layer,'Gmag'));
```

Appendix 4. Data processing: Plotting S_{11} and S_{21} of the transmission line

```
% Ploting the S11
figure(1)
plot(f,20*log10(abs(s11_1_layer(:))),'r','LineWidth',2)
hold on
plot(f,20*log10(abs(s11_2_layer(:))),'b','LineWidth',2)
hold on
plot(f,20*log10(abs(s11_3_layer(:))),'g','LineWidth',2)
% hold on
% plot(f,20*log10(abs(s11_4_layer(:))),'c','LineWidth',2)
xlabel('Frequency (Hz)')
ylabel('S11 (dB)')
legend('1 layer','2 layers','3 layers')
xlim([0.2e9 2e9]);
grid on

% Ploting S21
figure (2)
plot(f,20*log10(abs(s21_1_layer(:))),'r','LineWidth',2)
hold on
plot(f,20*log10(abs(s21_2_layer(:))),'b','LineWidth',2)
hold on
plot(f,20*log10(abs(s21_3_layer(:))),'g','LineWidth',2)
xlabel('Frequency (Hz)')
ylabel('S21 (dB)')
legend('1 layer','2 layers','3 layers')
grid on
```

Appendix 5. Data processing: Plotting max gain of the transmission line

```
% Ploting the max gain
figure(3)
plot(f,Gma_m_1_layer,'r','LineWidth',2);
hold on
plot(f,Gma_m_2_layer,'b','LineWidth',2);
hold on
plot(f,Gma_m_3_layer,'g','LineWidth',2);
xlabel('Frequency (Hz)')
ylabel('Max Gain (dB)')
legend('1 layer','2 layers','3 layers')
xlim([0.2e9 2e9]);
```